A Higher-Density Discrete Wavelet Transform

Ivan W. Selesnick, *Member, IEEE*

***Abstract*— This paper describes a new set of dyadic wavelet frames with two generators. The construction is simple, yet the wavelets cover the time-frequency plane in an arrangement that provides a higher sampling in both time and frequency. Specifically, the spectrum of the first wavelet is concentrated halfway between the spectrum of the second wavelet and the spectrum of its dilated version. In addition, the second wavelet is translated by half-integers rather than whole-integers in the frame construction. This arrangement leads to an expansive wavelet transform that is approximately shift-invariant and has intermediate scales. The wavelet frames presented in this paper are compactly supported and have vanishing moments.**

***Index Terms*— wavelet transform, frame, filter bank, shift-invariant.**

I. Introduction

VARIOUS types of wavelet transform are available for discrete data [6], [11]. Perhaps the most widely used discrete wavelet transform (DWT) is the critically-sampled DWT (implemented using FIR perfect reconstruction filter banks). Improved performance for some applications can be obtained by using an expansive (overcomplete, or redundant) transform. An expansive transform is one that expands an N-point signal to M transform coefficients with $M > N$. For example, the undecimated discrete wavelet transform (UDWT) [31] has been used for improved results for noise attenuation (denoising) [10], [20], deblocking of JPEG compressed images [37], and enhancement of chromosome images [35]. Other applications, for example edge detection, call for an approximation of the continuous wavelet transform [4].

Expansive wavelet transforms can be understood in part by examining how they sample the time-frequency plane. The critically-sampled DWT and undecimated DWT sample the time-frequency plane as illustrated in Fig. 1. The UDWT is shift-invariant, which has advantages as described in [32]. For the UDWT the temporal sampling is the same at each scale, which is inefficient for coarse scales (low frequency). When J scales are implemented, the UDWT is expansive by the factor $J + 1$. The double-density discrete wavelet transform [27], [28], which provides a compromise between the UDWT and the critically-sampled DWT, samples the time-frequency plane as shown in Fig. 1. The double-density DWT is two-times expansive, regardless of the number of scales implemented — potentially much less than the undecimated DWT. Even so, the double-density DWT is approximately shift-invariant. An alternative to the UDWT and double-density wavelet transform is the *partially* decimated wavelet transform (PWT) recently described in [33]. The redundancy of the PWT can be any integer from 1 to $J+1$ and the degree to which the transform is shift-invariant varies accordingly. None of these expansive transforms increase the sampling with respect to frequency (or scale). The scale-redundant DWT introduced in [21] has intermediate scales and can provide improved performance for denoising; however, that transform is undecimated (the temporal sampling is the same at each scale) and therefore highly redundant.

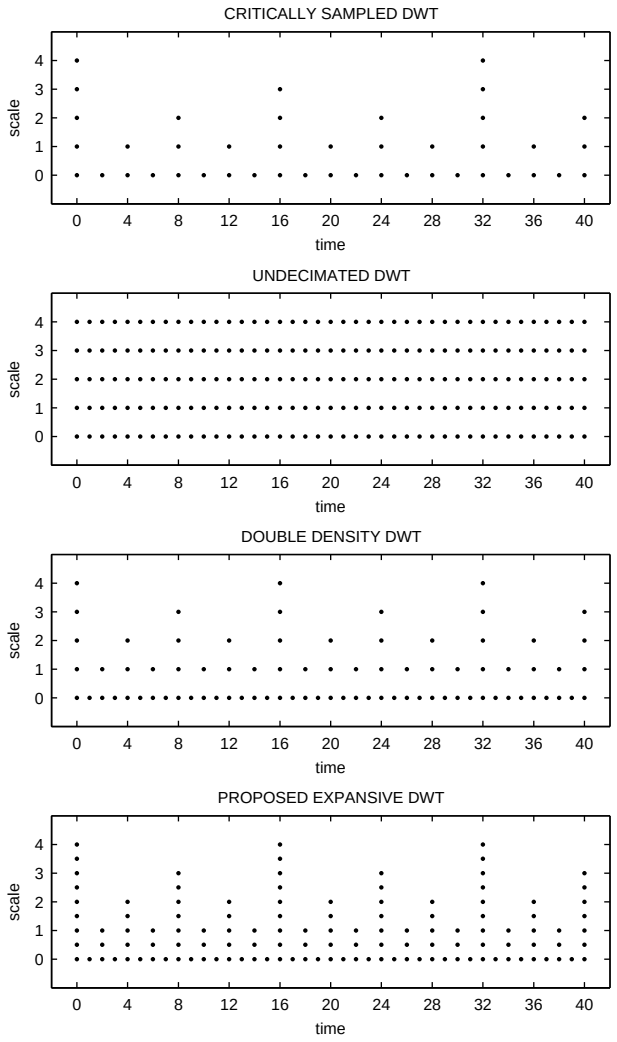

Fig. 1. Different discrete wavelet transforms sample the time-frequency plane in different ways. These diagrams are idealized — the actual sampling points may be offset from those shown here.

The Laplacian pyramid [7], in its one-dimensional form, corresponds to a sampling of the time-frequency plane like that of the double-density DWT. Recently, the Laplacian pyramid (LP) has been analyzed from a frame perspective [13]. The new reconstruction scheme proposed in [13] makes

The author is with the Department of Electrical and Computer Engineering, Polytechnic University, 6 Metrotech Center, Brooklyn, NY 11201. Email: selesi@poly.edu. Tel: (718) 260-3416. Fax: (718) 260-3906.

This work was supported by ONR under grant N00014-03-1-0217.

the LP a tight frame when orthonormal filters are used, or an approximately tight frame when nearly orthonormal filters (like the 9/7 pair) are used. The modification in [13] of the synthesis side of the LP is simple and provides significant improvement in applications.

This paper develops an expansive dyadic wavelet transform that oversamples both time and frequency by a factor of two. Like the double-density DWT, at each scale of the new transform there are twice as many coefficients as the critically-sampled DWT. However, the new transform also has intermediate scales; it has one scale between each pair of scales of the critically-sampled DWT. The way in which this transform samples the time-frequency plane is illustrated in the last panel of Fig. 1. The wavelet frame (or 'overcomplete' basis) associated with this expansive transform has two generators, $\psi_i(t)$, $i = 1, 2$. The spectrum of the the first wavelet is concentrated between the spectrum of the second wavelet and the spectrum of its dilated version [$\Psi_1(\omega)$ is concentrated between $\Psi_2(\omega)$ and $\Psi_2(2\,\omega)$]. In addition, the second wavelet is translated by integer multiples of one half, rather than whole integers. As this wavelet transform samples the time-frequency plane with a density that is three times the density of the non-expansive wavelet transform, this transform is expansive by a factor of three. This paper presents the construction of short compactly supported wavelets with vanishing moments for utilization with this transform. The transform can be implemented with digital filter banks like the conventional discrete wavelet transform.

Previously developed examples of dyadic wavelet frames generated by compactly supported wavelets (or 'affine frames') are given in [2], [8], [9], [12], [15], [17], [22], [23], [25]–[27], [30]. The theory, especially for tight frames from a multiresolution analysis, was established in [25] which also constructs the first set of spline tight frames. In [8] it was shown that given a compactly supported scaling function $\phi(t)$ not associated with any dyadic wavelet basis, it is often possible to obtain two compactly supported wavelets whose dyadic dilations and translations generate a tight frame. Issues addressed in these papers include the problem of the design of tight frames generated by (anti-) *symmetric* wavelets and the *maximization* of the number of vanishing moments. Briefly, imposing the symmetry constraint when there are three wavelets is substantially simpler than when there are only two [8], [17], [23], [30]. And when an IIR prefilter and/or postfilter is allowed, the number of vanishing moments of the wavelets can be increased by a number dependent on the scaling function (in a manner that is not possible for wavelet bases) [9], [12].

The family of wavelet frames proposed here is similar to those introduced in [1]. The type of wavelet frame developed in [1] also consists of two wavelets where one wavelet is half-integer translated, however, the associated filter is bandpass rather than highpass. Therefore, the associated sampling of the time-frequency plane is somewhat different than the one developed here. On the other hand, the wavelet frames in [1] have the advantage of being simultaneously tight and symmetric, unlike the frames proposed here.

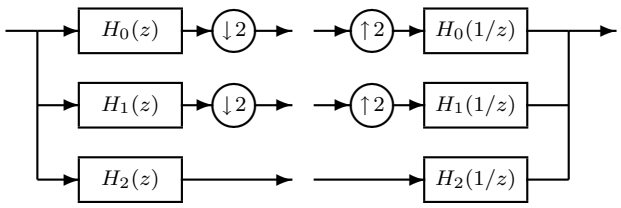

Fig. 2. The oversampled analysis and synthesis filter bank used for the implementation of the 3-times expansive wavelet transform.

II. Perfect Reconstruction Conditions

As in [25], following the multiresolution framework, the scaling function and two wavelets are defined through the dilation and wavelet equations:

$$\phi(t) = \sqrt{2} \sum_n h_0(n)\, \phi(2\,t - n) \tag{1}$$

$$\psi_i(t) = \sqrt{2} \sum_n h_i(n)\, \phi(2\,t - n), \quad i = 1, 2 \tag{2}$$

where $h_i(n)$, $n \in \mathbb{Z}$, are the filters of a digital filter bank. In this paper, we consider only real-valued $h_i(n)$ of compact support (FIR). The Z-transform of $h(n)$ is given by $H(z) = \sum_n h(n)\, z^{-n}$. The discrete-time Fourier transform of $h(n)$ is given by $H(e^{j\,\omega})$. If $h_i(n)$ satisfy the perfect reconstruction conditions given below and if $\phi(t)$ is sufficiently regular, then the dyadic dilations and translations of $\psi_i(t)$ form a tight frame for $L^2(\mathbb{R})$. Specifically, let $\phi_k(t) := \phi(t - k)$, $\psi_{1,j,k}(t) := \psi_1(2^j t - k)$ and $\psi_{2,j,k}(t) := \psi_2(2^j t - k/2)$. Then any square integrable signal $f(t)$ is given by

$$f(t) = \sum_{k=-\infty}^{\infty} c(k)\, \phi_k(t) + \sum_{i=1}^{2} \sum_{j=0}^{\infty} \sum_{k=-\infty}^{\infty} d_i(j,k)\, \psi_{i,j,k}(t)$$

where the expansion coefficients are given by

$$c(k) = \int f(t)\, \phi_k(t)\, dt \tag{3}$$

$$d_i(j,k) = \int f(t)\, \psi_{i,j,k}(t)\, dt, \quad i = 1, 2. \tag{4}$$

That is, the set of functions

$$\{\phi_k(t),\, \psi_{i,j,k}(t) \;\; : \;\; j, k \in \mathbb{Z},\; j \geq 0, \;\; i = 1, 2\}$$

form a tight frame for $L_2(\mathbb{R})$.

In order to achieve the sampling of the time-frequency plane illustrated in last panel of Fig. 1, we use the three-channel filter bank illustrated in Fig. 2 for the implementation of the transform. The first two channels are down-sampled by two while the third channel is undecimated.

To develop a set of filters that generate a tight wavelet frame, we will find conditions on the filters so the three-channel filter bank illustrated in Fig. 2 has the perfect reconstruction property. We will begin with a lowpass filter h_0 and a factorization of the transfer function $H_0(z)$ as a product $P(z)\, Q(z)$. From this factorization, we will determine the filters h_1 and h_2.

If the input and output signals in Fig. 2 are $x(n)$ and $y(n)$, then using standard multirate identities, the Z-transform of $y(n)$ is given by

$$\begin{aligned} Y(z) = {} & 0.5\,[H_0(z)\,X(z) + H_0(-z)\,X(-z)]\;H_0(1/z) \\ & + 0.5\,[H_1(z)\,X(z) + H_1(-z)\,X(-z)]\;H_1(1/z) \\ & + H_2(z)\,H_2(1/z)\,X(z). \end{aligned}$$

Rearranging gives $Y(z) = T(z)\,X(z) + V(z)\,X(-z)$ where $T(z)$ is given by

$$0.5\,[H_0(z)\,H_0(1/z) + H_1(z)\,H_1(1/z)] + H_2(z)\,H_2(1/z)$$

and $V(z)$ is given by

$$0.5\,[H_0(-z)\,H_0(1/z) + H_1(-z)\,H_1(1/z)].$$

Therefore, for perfect reconstruction (PR), we need

$$H_0(z)\,H_0(1/z) + H_1(z)\,H_1(1/z) + 2\,H_2(z)\,H_2(1/z) = 2 \quad (5)$$

and

$$H_0(-z)\,H_0(1/z) + H_1(-z)\,H_1(1/z) = 0. \quad (6)$$

To derive filters h_0, h_1, h_2 satisfying the PR conditions, let us factor $H_0(z)$ as

$$H_0(z) = P(z)\,Q(z). \quad (7)$$

The degree of $Q(z)$ will be denoted by L. Define

$$H_1(z) := z^{-\alpha}\,P(z)\,Q(-1/z)\,(-z)^{-L} \quad (8)$$

where

$$\alpha = \begin{cases} 0, & \text{if } L \text{ is odd} \\ 1, & \text{if } L \text{ is even.} \end{cases} \quad (9)$$

Then $\alpha + L$ will be odd. Using (7) and (8) it follows that $H_1(-z)\,H_1(1/z) = -H_0(-z)\,H_0(1/z)$ (the derivation of this identity uses the fact that $\alpha + L$ is odd). That means, the second of the two PR conditions (6) is satisfied. Now we have only to find $H_2(z)$ so as to satisfy (5), the first of the two PR conditions. To find $H_2(z)$, we use (5) to write

$$\begin{aligned} & H_2(z)\,H_2(1/z) \\ & \quad = \frac{1}{2}\,[2 - H_0(z)\,H_0(1/z) - H_1(z)\,H_1(1/z)]. \end{aligned} \quad (10)$$

Provided that the right hand side of (10) is nonnegative on the unit circle $z = e^{j\omega}$, the filter $H_2(z)$ can be obtained via spectral factorization.

The set of filters therefore follows from the lowpass filter h_0 and a particular factorization of its transfer function. The choice of lowpass filter and its factorization is addressed in the next section.

III. Framelets with Vanishing Moments

In this paper, we are interested in constructing wavelets with vanishing moments. The vanishing moments of the wavelets and the approximation order of the scaling function depend directly on the multiplicity of the zero at $z = -1$ of the transfer function $H_0(z)$, and on the multiplicity of the zero at $z = 1$ of the transfer functions $H_1(z)$ and $H_2(z)$. In the following we examine the multiplicity of these zeros and propose a specific factorization of $H_0(z)$.

Suppose the lowpass filter $H_0(z)$ possesses K_0 zeros at $z = -1$,

$$H_0(z) = \left(\frac{1 + z^{-1}}{2}\right)^{K_0} A(z) \quad (11)$$

and satisfies $H(1) = \sqrt{2}$. (This normalization is required in order that the wavelets be well defined and is the same normalization used in the construction of orthonormal wavelet bases.) The degree of $A(z)$ is denoted by M.

Then $2 - H_0(z)\,H_0(1/z)$ will be a highpass filter. Let us factor out the roots at $z = 1$. If $2 - H_0(z)\,H_0(1/z)$ has $2\,K_2$ roots at $z = 1$, we can write

$$\begin{aligned} & 2 - H_0(z)\,H_0(1/z) \\ & \qquad = \left(\frac{-z + 2 - z^{-1}}{4}\right)^{K_2} B(z)\,B(1/z) \end{aligned} \quad (12)$$

for some $B(z)$. Assuming $K_0 > K_2$, let us factor $H_0(z)$ as $P(z)\,Q(z)$ where

$$P(z) = \left(\frac{1 + z^{-1}}{2}\right)^{K_1} \quad (13)$$

$$Q(z) = \left(\frac{1 + z^{-1}}{2}\right)^{K_2} A(z) \quad (14)$$

where $K_0 = K_1 + K_2$. The degree of $Q(z)$, denoted by L, is $L = K_2 + M$. Then from (8), (13), and (14), we have

$$\begin{aligned} H_1(z) = z^{-\alpha} & \left(\frac{1 + z^{-1}}{2}\right)^{K_1} \left(\frac{1 - z^{-1}}{2}\right)^{K_2} \\ & \times A(-1/z)\,(-z)^{-M}. \end{aligned} \quad (15)$$

The filter $H_2(z)$ is then found using (10). Specifically, using (12) and (15), $H_2(z)\,H_2(1/z)$ is given by

$$H_2(z)\,H_2(1/z) = \frac{1}{2}\left(\frac{-z + 2 - z^{-1}}{4}\right)^{K_2} C_r(z) \quad (16)$$

where $C_r(z)$ is defined as

$$C_r(z) := B(z)\,B(1/z) - \left(\frac{z + 2 + z^{-1}}{4}\right)^{K_1} A(-z)\,A(-1/z).$$

Then we can write

$$H_2(z) = \frac{1}{\sqrt{2}}\left(\frac{1 - z^{-1}}{2}\right)^{K_2} C(z) \quad (17)$$

where $C(z)$ is a spectral factor of $C_r(z)$,

$$C(z)\,C(1/z) := C_r(z). \quad (18)$$

This does not uniquely determine $C(z)$ because several distinct spectral factorizations are possible in general. In summary we have

$$H_0(z) = \left(\frac{1 + z^{-1}}{2}\right)^{K_0} A(z) \quad (19)$$

$$\begin{aligned} H_1(z) = z^{-\alpha} & \left(\frac{1 + z^{-1}}{2}\right)^{K_1} \left(\frac{1 - z^{-1}}{2}\right)^{K_2} \\ & \times A(-1/z)\,(-z)^{-M} \end{aligned} \quad (20)$$

$$H_2(z) = \frac{1}{\sqrt{2}}\left(\frac{1 - z^{-1}}{2}\right)^{K_2} C(z). \quad (21)$$

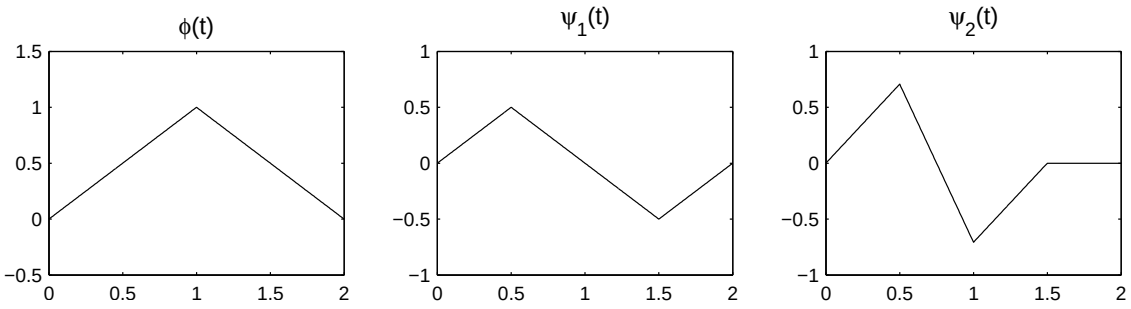

Fig. 3. Example 1 — Tight frame with 1 vanishing moment. $K_0 = 2$, $K_1 = 1$, $K_2 = 1$.

Note in particular that $H_1(z)$ and $H_2(z)$ each have the factor $(1-z^{-1})^{K_2}$. Therefore, each of these two channels of the filter bank annihilate discrete-time polynomial signals up to degree $K_2 - 1$. Correspondingly, the wavelets $\psi_1(t)$ and $\psi_2(t)$ each have K_2 vanishing moments.

A. Minimal-length Solutions

To construct short wavelets with vanishing moments we seek solutions of minimal length, subject to the number of vanishing moments K_2 and parameter K_0. The parameter K_0, see equation (11), affects the regularity of the scaling function $\phi(t)$. The parameter K_2 is the number of vanishing moments shared by the wavelets $\psi_1(t)$ and $\psi_2(t)$. (One of the wavelets may have more vanishing moments than the other, but each is guaranteed to have at least K_2 vanishing moments).

Let $F(z) := H_0(z)\,H_0(1/z)$. Then $f(n)$ is a symmetric odd-length filter (a Type-I linear-phase FIR filter). From equations (11) and (12), it is required that $F(z)$ has a zero at $z = -1$ of multiplicity $2\,K_0$ and that $2 - F(z)$ has a zero at $z = 1$ of multiplicity $2\,K_2$. To obtain wavelets with minimal support, we seek the shortest such filter $f(n)$. The solution to this problem is the *maximally-flat* linear-phase FIR filter, a family of filters described by Herrmann [16]. The filter $H_0(z)$ is obtained from $F(z)$ by spectral factorization. The formula for $F(z) = H_0(z)\,H_0(1/z)$ provided by Herrmann is

$$F(z) = 2\left(\frac{z+2+z^{-1}}{4}\right)^{K_0} \times \sum_{k=0}^{K_2-1} \binom{K_0-1+k}{k} \left(\frac{-z+2-z^{-1}}{4}\right)^{k}. \quad (22)$$

When $K_0 = K_2$, this formula specializes to the filter used for the construction of Daubechies orthonormal wavelets [11].

B. Example 1

The simplest example is obtained by setting $K_1 = 1$ and $K_2 = 1$. Then $K_0 = K_1 + K_2 = 2$ and the filters are given by,

$$h_0 = \frac{\sqrt{2}}{4}\,[1, \quad 2, \quad 1]$$

$$h_1 = \frac{\sqrt{2}}{4}\,[1, \quad 0, \quad -1]$$

$$h_2 = \frac{1}{2}\,[1, \quad -1, \quad 0]$$

for $0 \le n \le 2$. In this example, the scaling function and wavelets are piecewise linear, continuous and (anti-) symmetric, as illustrated in Fig. 3. Both wavelets have only one vanishing moment. In the following examples, where $K_2 > 1$, the wavelets do not have a closed form solution and are not (anti-) symmetric.

C. Example 2

In this example we set $K_1 = 1$ and $K_2 = 3$. Then $K_0 = K_1 + K_2 = 4$. With these parameters we have from (22)

$$F(z) = \left(\frac{z+2+z^{-1}}{4}\right)^4 \times \left(13.5 - 7\,(z+z^{-1}) + 1.25\,(z^2+z^{-2})\right).$$

Performing spectral factorization to get $H_0(z)$ from $F(z) = H_0(z)\,H_0(1/z)$ gives

$$H_0(z) = \left(\frac{1+z^{-1}}{2}\right)^4 \left(3.0337 - 2.0315\,z^{-1} + 0.4120\,z^{-2}\right).$$

From (15),

$$H_1(z) = \left(\frac{1+z^{-1}}{2}\right)\left(\frac{1-z^{-1}}{2}\right)^3 \times \left(0.4120 + 2.0315\,z^{-1} + 3.0337\,z^{-2}\right).$$

The filter $H_2(z)$ can be found from spectral factorization. From (16)

$$H_2(z)\,H_2(1/z) = \frac{1}{2}\left(\frac{-z+2-z^{-1}}{4}\right)^4 \times \left(5.5 + 2\,(z+z^{-1}) + 0.25\,(z^2+z^{-2})\right)$$

so

$$H_2(z) = \frac{1}{\sqrt{2}}\left(\frac{1-z^{-1}}{2}\right)^4 \times \left(0.1150 + 0.8740\,z^{-1} + 2.1732\,z^{-2}\right).$$

The filter coefficients are listed in Table I. Fig. 4 illustrates the filters, the scaling function $\phi(t)$, and wavelets $\psi_1(t)$ and $\psi_2(t)$. The filter h_1 is the bandpass filter, while h_2 is the highpass filter; the frequency responses of the filters are illustrated in Fig. 5. The wavelets have three vanishing moments each. The

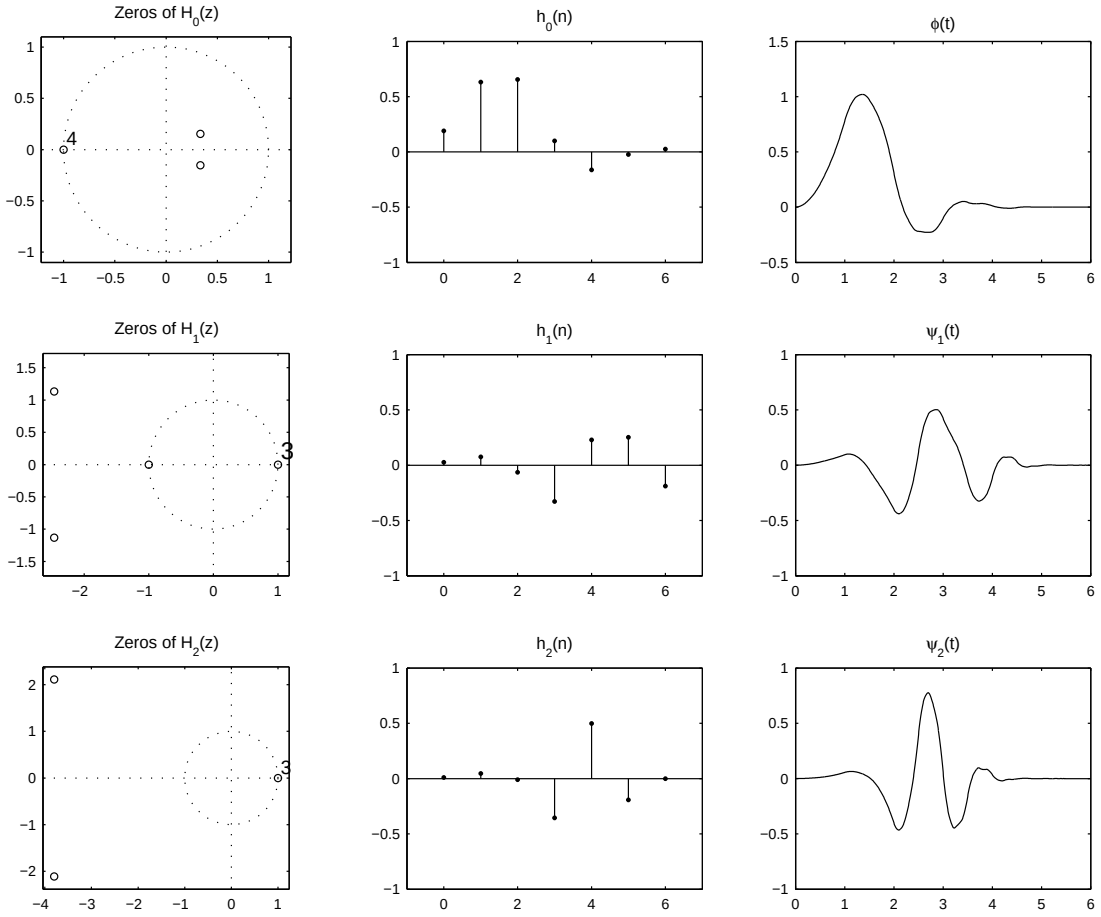

Fig. 4. Example 2 — Tight frame with 3 vanishing moments. $K_0 = 4$, $K_1 = 1$, $K_2 = 3$.

TABLE I
COEFFICIENTS FOR EXAMPLE 2.

n	$h_0(n)$	$h_1(n)$	$h_2(n)$
0	0.189604909379	0.025752563665	0.010167956157
1	0.631450512121	0.075463998066	0.046750380120
2	0.655505518357	-0.064333341412	-0.009172584871
3	0.099615139800	-0.327704691428	-0.354664087684
4	-0.163756210215	0.228185687127	0.499004628714
5	-0.023958870736	0.252240693362	-0.192086292435
6	0.025752563665	-0.189604909379	0

wavelet $\psi_1(t)$ has support 6, while the wavelet $\psi_2(t)$ has support 5.5.

Fig. 6 compares the frequency responses of the 3-stage critically-sampled wavelet transform and the 3-stage proposed expansive wavelet transform. As the figure illustrates, the proposed expansive DWT has more subbands than the critically-sampled DWT, but it maintains the same octave-type frequency decomposition that is characteristic of that transform. Note that the frequency response of each subband (excepting the lowpass subband) of the proposed transform has a reduced gain compared to those of the critically-sampled DWT. That normalization is due to the higher sampling rate of each subband of the proposed transform.

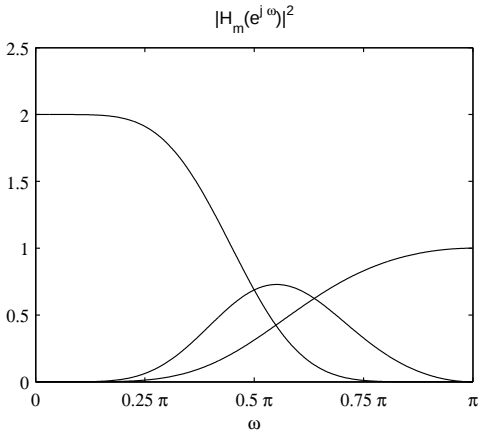

Fig. 5. The frequency responses of h_0, h_1, h_2 in Example 2.

Because $H_0(z)$ has $(1+z^{-1})^4$ as a factor, while $H_1(z)$ and $H_2(z)$ each have only $(1-z^{-1})^3$ as a factor, the wavelets are more regular than the Daubechies orthonormal wavelets with three vanishing moments. To be precise, the Sobolev regularity parameter for the wavelets shown in Fig. 4 is 2.17, while the Daubechies wavelets with three vanishing moments have a Sobolev exponent of 1.42. Note that the filters in Example 2 are of length 7, while the Daubechies filters are

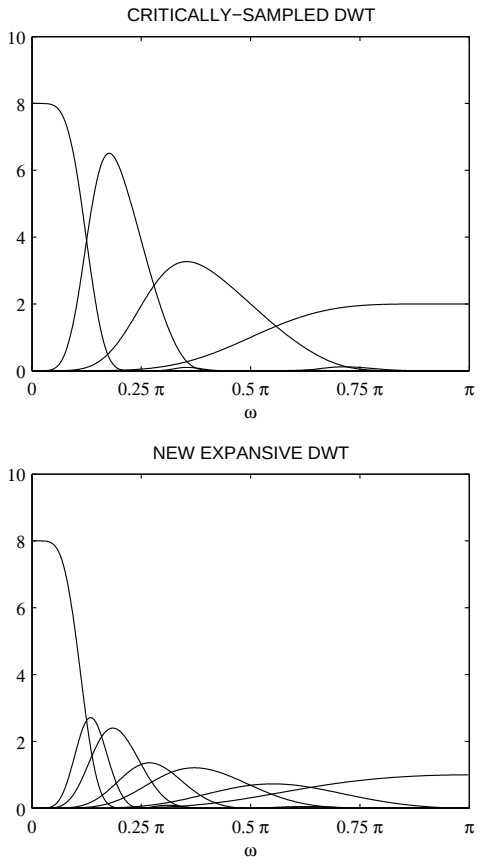

Fig. 6. The frequency responses of the three-stage discrete wavelet transform. Top: critically-sampled DWT using Daubechies 6-tap filters (3 vanishing moments). Bottom: over-sampled DWT using filters of Example 2 (3 vanishing moments).

of length 6, so the additional smoothness may come from the increased filter length. However, the Daubechies filter of length 8 (generating wavelets with 4 vanishing moments) has a Sobolev exponent of 1.78, still less than the proposed wavelets. Table II tabulates the Sobolev exponents for the Daubechies orthonormal wavelets and the proposed wavelets for different numbers of vanishing moments. Although the proposed wavelet frame is designed so as to provide a denser sampling of the time-frequency plane, a positive side effect is an increase in the smoothness of the wavelets.

D. Example 3

In this example we set $K_1 = 1$ and $K_2 = 4$. Then $K_0 = K_1 + K_2 = 5$. The filters, scaling function $\phi(t)$ and wavelets $\psi_1(t)$ and $\psi_2(t)$ are illustrated in Fig. 7. The wavelet $\psi_1(t)$ has support 8, while the wavelet $\psi_2(t)$ has support 7.5. The wavelets have four vanishing moments each and the Sobolev regularity parameter is 2.48. In this example, a mid-phase spectral factorization was used to obtain a more symmetric solution than that obtained with a minimum-phase solution. The filter coefficients are listed in Table III.

E. Example 4

In this example we set $K_1 = 3$ and $K_2 = 2$. The wavelets, illustrated in Fig. 8, have two vanishing moments each. The

TABLE II

COMPARISON OF SOBOLEV REGULARITY EXPONENT AND SUPPORT. K IS THE NUMBER OF VANISHING MOMENTS. THE PROPOSED WAVELETS HAVE $K_1 = 1$ AND $K_2 = K$.

	Ortho Daubechies		Proposed tight frame	
K	*Sobolev*	*Supp.* $\psi(t)$	*Sobolev*	*Supp.* $\psi_1(t)$, $\psi_2(t)$
1	0.50	1	1.50	2, 1.5
2	1.00	3	1.84	4, 3.5
3	1.42	5	2.17	6, 5.5
4	1.78	7	2.48	8, 7.5
5	2.10	9	2.77	10, 9.5
6	2.39	11	3.03	12, 11.5
7	2.66	13	3.28	14, 13.5
8	2.91	15	3.52	16, 15.5
9	3.16	17	3.76	18, 17.5
10	3.40	19	3.99	20, 19.5

TABLE III

COEFFICIENTS FOR EXAMPLE 3.

n	$h_0(n)$	$h_1(n)$	$h_2(n)$
0	0.022033327573	0.048477254777	0.031294135831
1	0.015381522616	0.019991451948	0.013248398005
2	-0.088169084245	-0.304530024033	-0.311552292833
3	0.051120949834	0.165478923930	0.497594326648
4	0.574161374258	0.308884916012	-0.235117092484
5	0.717567366340	-0.214155508410	-0.020594576659
6	0.247558418377	-0.074865474330	0.015375249485
7	-0.076963057605	0.028685132531	0.009751852004
8	-0.048477254777	0.022033327573	0

Sobolev exponent of the wavelets is 3.60, substantially higher than the previous examples even though the filters h_0 and h_1 are only of length 7 and h_2 is of length 6. Increasing the value of the parameter K_1 increases the regularity of the wavelets; however, it also reduces the norm of the filter h_1. The filter h_1 is small in norm compared to h_2. This is especially noticeable in the frequency response plot, Fig. 9. Precisely, the norm of h_1 is 0.30, while the norm of h_2 is 0.78. For comparison, the norms of the filters h_1 and h_2 in Example 3 are 0.52 and 0.63. Although it is not necessary that the filter norms be equal for the frame to be tight, the large difference in norms means that the expansive transform is somewhat inefficient and the dense sampling of the time-frequency grid is not fully utilized. In the extreme case where the norm of h_1 is (close to) zero, that filter could be omitted altogether. One may as well use, in that case, the double-density discrete wavelet transform, or another transform that is overcomplete by a factor of two.

The reduced norm of h_1 is explained using the second perfect reconstruction condition (6) and setting $\omega = 0.5\,\pi$. From (6) it follows that

$$|H_0(e^{j\,0.5\,\pi})| = |H_1(e^{j\,0.5\,\pi})|. \tag{23}$$

That the magnitude of the frequency response of h_0 and h_1 are equal at $\omega = 0.5\,\pi$ can be seen in Figs. 4 and 8. In addition, increasing the value of K_1 makes the passband of $H_0(e^{j\,\omega})$ narrower and reduces its value at $\omega = 0.5\,\pi$. From

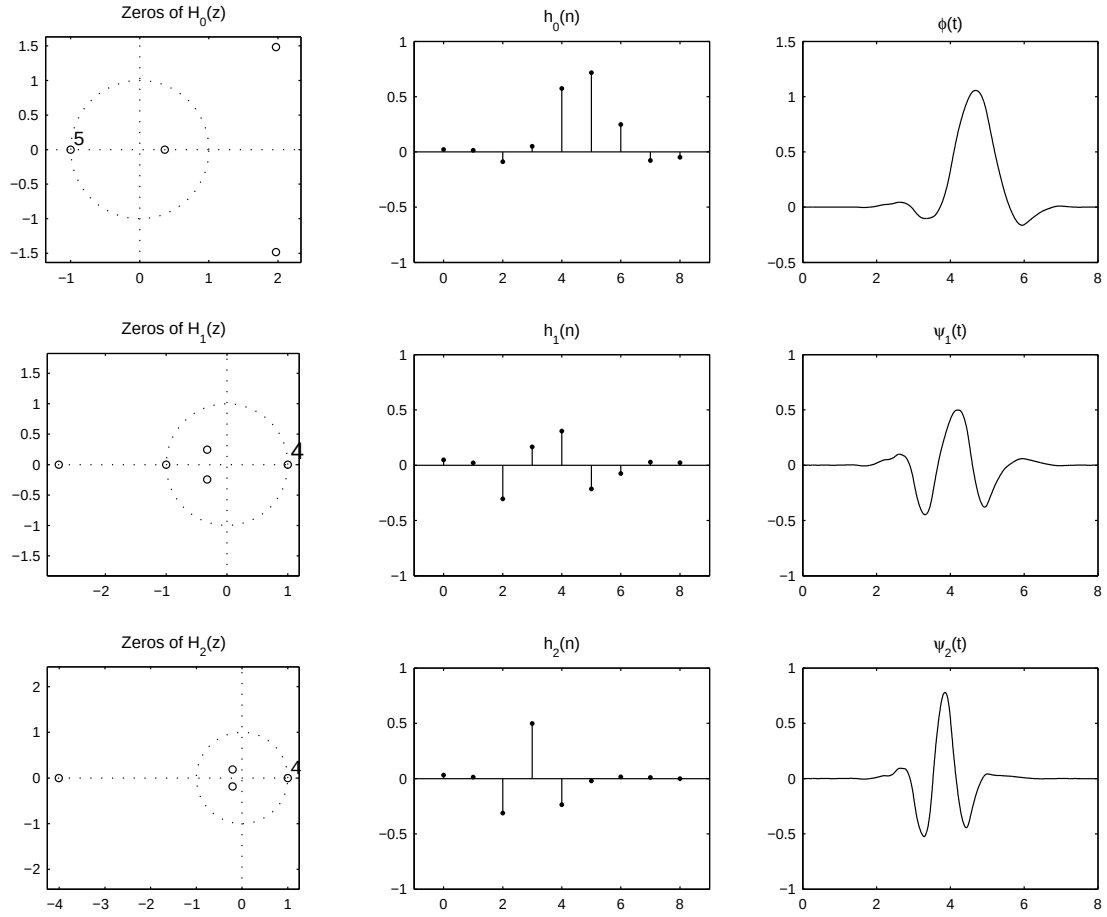

Fig. 7. Example 3 — Tight frame with 4 vanishing moments. $K_0 = 5$, $K_1 = 1$, $K_2 = 4$.

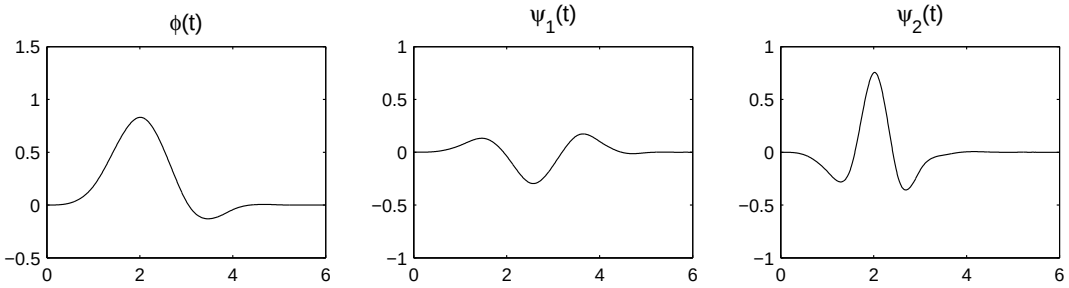

Fig. 8. Example 4 — Tight frame with 3 vanishing moments. $K_0 = 5$, $K_1 = 3$, $K_2 = 2$.

(23), the bandpass filter $H_1(e^{j\,\omega})$ must also have a small value at $\omega = 0.5\,\pi$, as illustrated in Fig. 8. For that reason, increasing the value of the parameter K_1 reduces the norm of h_1. We therefore suggest setting K_1 equal to one. For $K_1 = 1$, the norms of the $\psi_1(t)$ and $\psi_2(t)$ are closer in value, as in Examples 2 and 3.

F. Fractional Dilation Parameters

Non-dyadic wavelet transforms have been investigated in the literature. In this case, the dilation equation is given by

$$\phi(t) = \sqrt{a}\,\sum_n h_0(n)\,\phi(a\,t - n)$$

where a is different from 2. When a is an integer greater than two, solving the dilation equation for $\phi(t)$ is quite straightforward, and one can develop associated wavelet transforms [34], [36]. When a is a non-integer, then solving the dilation equation and developing an associated wavelet transform is much more complicated [5]. The case where a is between 1 and 2 is interesting because in this case stepping between scales is more gradual. In terms of sampling of the time-frequency plane, allowing a to be between 1 and 2 gives a closer spacing of the samples with respect to frequency. However, it is difficult to implement a discrete wavelet transform based on $1 < a < 2$. Although the wavelet frame proposed here is not associated with any such fractional dilation factor,

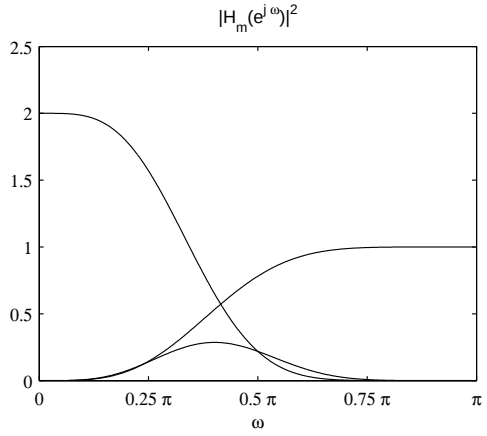

Fig. 9. The frequency responses of h_0, h_1, h_2 in Example 4.

it does provide a denser sampling of the time-frequency plane, and intermediate scales, as illustrated in Fig. 6.

IV. Bi-Frames and Symmetry

The widely used symmetric biorthogonal 9/7 wavelet basis is obtained by relaxing the orthogonality constraint [3]. Similarly, wavelet frames with (anti-) symmetric scaling functions and wavelets can be easily obtained by relaxing the tightness of the frame. Equivalently, by allowing the synthesis filters and analysis filters to be different from each other, we can obtain a perfect reconstruction filter bank with (anti-) symmetric filters. In this case, the perfect reconstruction conditions become

$$H_0(z)\,\tilde{H}_0(z) + H_1(z)\,\tilde{H}_1(z) + 2\,H_2(z)\,\tilde{H}_2(z) = 2\,z^{-n_o} \tag{24}$$

$$H_0(-z)\,\tilde{H}_0(z) + H_1(-z)\,\tilde{H}_1(z) = 0 \tag{25}$$

where a delay of n_o samples is specified in the reconstruction [$y(n) = x(n - n_o)$]. The filters H_i are the analysis filters, while $\tilde{H}_i$ are the synthesis filters.

Similar to the factorizations presented above for the tight frame case, we define the following factorization for $H_0(z)$ and corresponding factorizations for other transfer functions,

$$H_0(z) = P(z)\,Q(z) \tag{26}$$

$$\tilde{H}_0(z) = \tilde{P}(z)\,\tilde{Q}(z) \tag{27}$$

$$H_1(z) = P(z)\,\tilde{Q}(-z)\,(-z)^d \tag{28}$$

$$\tilde{H}_1(z) = -\tilde{P}(z)\,Q(-z)\,z^{-d} \tag{29}$$

With the transfer functions related in this way, the second perfect reconstruction condition (25) is satisfied, regardless of the actual transfer functions $P(z)$ and $Q(z)$.

To obtain $H_2(z)$ and $\tilde{H}_2(z)$ we can write the first perfect reconstruction condition (24) as

$$H_2(z)\,\tilde{H}_2(z) = z^{-n_o} - \frac{1}{2}\,P(z)\,\tilde{P}(z) \times \left[Q(z)\,\tilde{Q}(z) - (-1)^d\,Q(-z)\,\tilde{Q}(-z)\right].$$

The transfer functions $H_2(z)$ and $\tilde{H}_2(z)$ can now be obtained by factorization of the right-hand-side.

TABLE V
Comparison of Sobolev regularity exponents.

	9/7 biorthogonal	Example 5
analysis	1.41	2.00
synthesis	2.12	2.94

Recall that the biorthogonal symmetric 9/7 wavelet basis and the Daubechies-8 orthonormal wavelet basis with four vanishing moments are obtained by different factorizations of the same filter (a maximally-flat symmetric FIR halfband filter). Likewise, we propose to design short symmetric wavelets with vanishing moments by setting the product $H_0(z)\,\tilde{H}_0(z)$ equal to the same maximally-flat filter $F(z)$ in (22) that we used for the design of tight wavelet frames in Section III.

As in Section III, we propose setting

$$P(z) = \tilde{P}(z) = \left(\frac{1+z^{-1}}{2}\right)^{K_1}$$

and

$$Q(z) = \left(\frac{1+z^{-1}}{2}\right)^{K_2} A(z)$$

$$\tilde{Q}(z) = \left(\frac{1+z^{-1}}{2}\right)^{K_2} \tilde{A}(z).$$

We further suggest setting K_1 equal to 1 for the reason noted in Example 4.

A. Example 5

A non-tight wavelet frame with symmetric filters is obtained in this example by performing factorizations into symmetric filters, starting with the lowpass filter $F(z)$ used in Example 3. The analysis and synthesis wavelets are illustrated in Figs. 10 and 11 respectively. The filter coefficients are listed in Table IV. To make the filters causal, the delay in the perfect reconstruction is $n_o = 8$ samples, $y(n) = x(n - 8)$. The analysis wavelets are supported on $[0,\ 8]$ and $[0.5,\ 8]$, while the synthesis wavelets are supported on $[0,\ 8]$ and $[0,\ 7.5]$. Both analysis wavelets and both synthesis wavelets have four vanishing moments. Like the biorthogonal 9/7 system, the synthesis scaling function is shorter and smoother than the analysis scaling function. The wavelets constructed in this example are more regular than the 9/7 biorthogonal wavelets, because the lowpass filters each have $(1 + z^{-1})^5$ as a factor. Table V lists the Sobolev regularity exponents of the designed wavelets and the 9/7 wavelets.

Note that the zeros of $H_0(z)$ and $\tilde{H}_0(z)$ as illustrated in Figs. 10 and 11 have the same type of configuration as the biorthogonal 9/7 filters. Namely, the analysis lowpass filter has four complex zeros away from $z = -1$, while the synthesis lowpass filter has two real zeros away from $z = -1$. Unlike the biorthogonal 9/7 filters, the lengths of the filters in Figs. 10 and 11 do not all have the same parity. The lowpass and bandpass filters are even-length while the highpass filters are odd-length. Furthermore, the even-length filters do not have the same center of symmetry, and as a consequence the implementation of symmetric boundary extensions must be

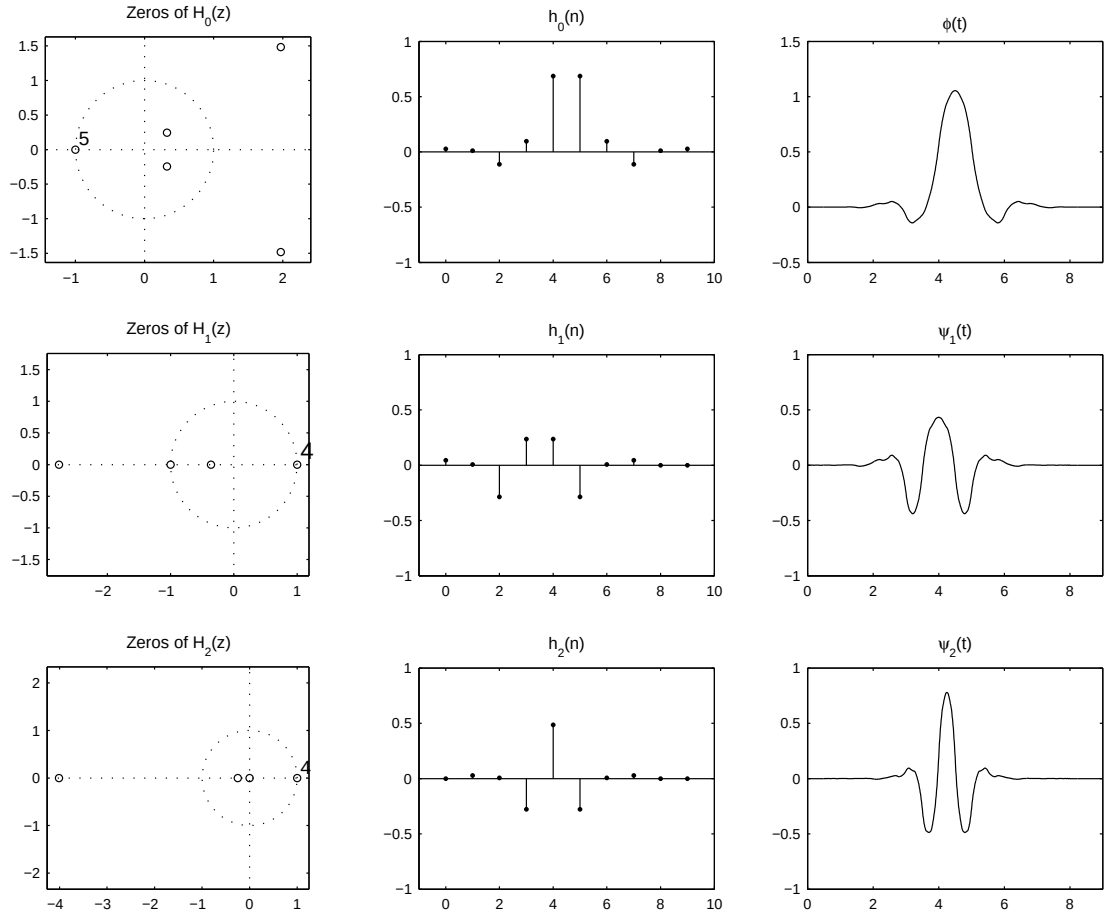

Fig. 10. Example 5 — Symmetric analysis filters and wavelets with four vanishing moments. $K_0 = 5$, $K_1 = 1$, $K_2 = 4$.

TABLE IV
COEFFICIENTS FOR EXAMPLE 5.

n	$h_0(n)$	$h_1(n)$	$h_2(n)$	$\tilde{h}_0(n)$	$\tilde{h}_1(n)$	$\tilde{h}_2(n)$
0	0.027222	0.044889	0	-0.039237	0.023794	0.011029
1	0.011217	0.005671	0.027671	-0.073518	0.037784	0.019204
2	-0.112709	-0.286349	0.007159	0.181733	-0.070538	-0.020024
3	0.096078	0.235789	-0.277671	0.638129	-0.253037	-0.269204
4	0.685299	0.235789	0.485682	0.638129	0.261996	0.517991
5	0.685299	-0.286349	-0.277671	0.181733	0.261996	-0.269204
6	0.096078	0.005671	0.007159	-0.073518	-0.253037	-0.020024
7	-0.112709	0.044889	0.027671	-0.039237	-0.070538	0.019204
8	0.011217	0	0	0	0.037784	0.011029
9	0.027222	0	0	0	0.023794	0

slightly different than that for symmetric biorthogonal wavelet transforms. Specifically, if the input signal to the analysis filter bank (see Fig. 2) has length N (where N is even) and if symmetric boundary conditions are implemented, then the lowpass, bandpass, and highpass subband signals require $N/2$, $N/2 + 1$, and N samples respectively. That is, the bandpass subband requires one more sample than initially expected. Because the transform is already expansive, the 'extra' sample in the bandpass subband required for the implementation of symmetric boundary conditions is not of consequence.

V. APPLICATION TO SIGNAL DENOISING

To evaluate the proposed 3-times expansive wavelet transform we have used it for 1-D signal denoising and compared it with the critically-sampled DWT, the double-density DWT and the undecimated DWT. The root-mean-square error is calculated as a function of the threshold value used in the denoising procedure. The result of the denoising experiment is shown in Fig. 12. The performance of the proposed transform is nearly that of the UDWT, yet it is only 3-times expansive whereas the UDWT is 6-times expansive. The details of the denoising experiment are as follows.

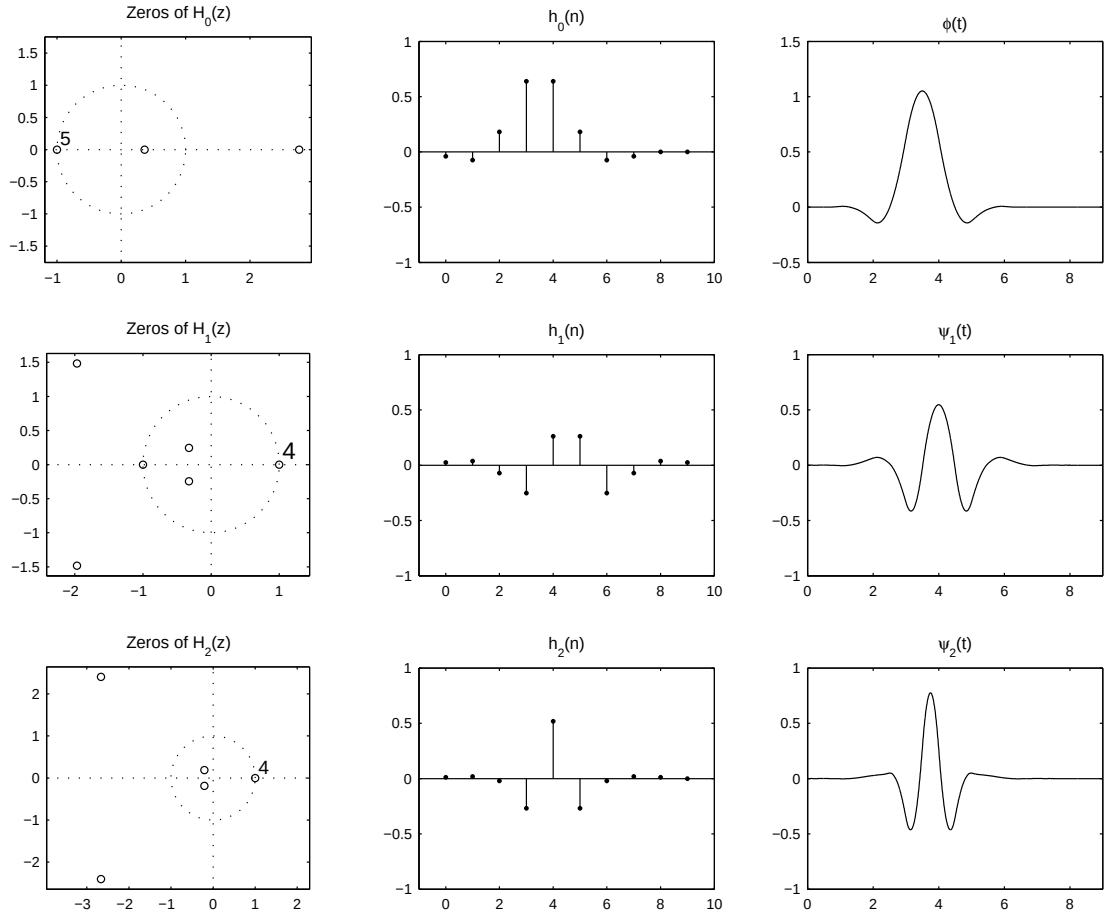

Fig. 11. Example 5 — Symmetric synthesis filters and wavelets with four vanishing moments. $K_0 = 5$, $K_1 = 1$, $K_2 = 4$.

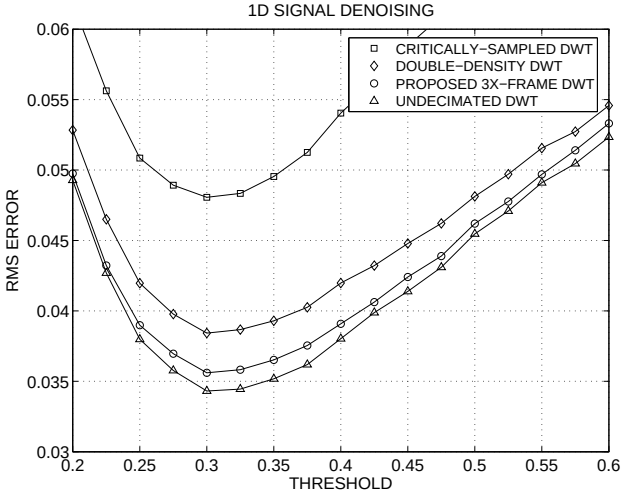

Fig. 12. Comparison of denoising performance. The proposed 3-times expansive wavelet transforms performs nearly as well as the more expansive undecimated wavelet transform.

For the proposed transform we used the filters presented in Example 2 with three vanishing moments; for the critically-sampled and undecimated DWT we used the orthonormal Daubechies wavelets with three vanishing moments. For the double-density DWT we used the wavelets from [27] with three vanishing moments. For each transform we used five stages. We used a 1024-point signal from the `WaveLab` software package [14], produced using the command `MakeSignal('Piece-Regular',1024)`. The signal was normalized so that its maximum value was 1 and independent white zero-mean Gaussian random noise with standard deviation of 0.1 was added. We used the hard threshold rule on every subband except the lowpass subband. For the proposed transform, the threshold, T, was multiplied by the norm of the filter response for that subband prior to thresholding. This is necessary because the wavelets of the proposed transform do not have the same norm and moreover, the norm depends on the scale. The results illustrated in Fig. 12 were obtained from averaging over 200 realizations. In another denoising experiment, the best performing threshold per subband was chosen for all transforms, and in this case the difference between the proposed expansive transform and the UDWT was further reduced.

VI. Two-Dimensional Transforms

The proposed expansive wavelet transform can be extended to multiple dimensions in a way that is similar to the usual separable implementation. For two-dimensional signals there will be eight subbands at each stage: LB, LH, BL, BB, BH, HL, HB, HH, where L stands for ‘lowpass’, H stands for

TABLE VI
RELATIVE SIZES OF SUBBANDS FOR THE 2-D TRANSFORM.

LB	$N \times N$
LH	$N \times 2\,N$
BL	$N \times N$
BB	$N \times N$
BH	$N \times 2\,N$
HL	$2\,N \times N$
HB	$2\,N \times N$
HB	$2\,N \times 2\,N$
Total	$15\,(N \times N)$

'highpass', and B stands for 'bandpass'. These are in addition to the LL subband. If the LL subband is of size $N \times N$, then the LH subband will be of size $N \times 2N$, the HH subband will be of size $2N \times 2N$, etc. Table VI shows the relative sizes of each subband. In comparison, the critically-sampled two-dimensional DWT has three subbands, LH, HL, HH, each of size $N \times N$. Therefore, the 2-D form of the proposed transform is 5-times expansive. That can potentially be substantially less than the 2-D form of the the undecimated DWT, which is $(3\,J + 1)$-times expansive, where J is the number of stages.

VII. CONCLUSION

This paper has presented a type of discrete wavelet transform that is overcomplete by a factor of 3 (by a factor of 5 for two-dimensional signals). A family of tight wavelet frames were presented that have minimal-length for a specified number of vanishing moments. The construction of the filters requires the spectral factorization of a maximally-flat lowpass linear-phase FIR filter (as does the construction of orthonormal Daubechies wavelets) and one additional spectral factorization. In addition, the design of non-tight frames generated by symmetric wavelets was also presented.

Several variations and extensions of this work are possible. For example, the lowpass filter h_0 need not be the spectral factor of a maximally-flat linear-phase FIR filter — instead h_0 can itself be such a filter. In this case, both h_0 and h_1 will be (anti-) symmetric.

Another extension is the development of a dual-tree complex (approximately analytic) wavelet transform [18], [19] based on the type of filter bank used in this paper. A complex form of the double-density DWT was presented in [29].

Software to implement the transform and reproduce the design examples is available on the web at `http://taco.poly.edu/selesi/`.

ACKNOWLEDGMENT

The author thanks A. Farras Abdelnour for fruitful discussions.

REFERENCES

[1] A. F. Abdelnour. Symmetric tight frame with shifted wavelets. In *Wavelets XI, Proc. SPIE 5914*, San Diego, 2005.

[2] A. F. Abdelnour and I. W. Selesnick. Symmetric nearly shift-invariant tight frame wavelets. *IEEE Trans. on Signal Processing*, 53(1):231–239, January 2005.

[3] M. Antonini, M. Barlaud, P. Mathieu, and I. Daubechies. Image coding using wavelet transforms. *IEEE Trans. on Image Processing*, 1(2):205–220, April 1992.

[4] K. Berkner and R. O. Wells, Jr. A new hierarchical scheme for approximating the continuous wavelet transform with applications to edge detection. *IEEE Signal Processing Letters*, 6(8):193–195, August 1999.

[5] T. Blu. Iterated filter banks with rational rate changes connection with discrete wavelet transforms. *IEEE Trans. on Signal Processing*, 41(12):3232–3244, December 1993.

[6] C. S. Burrus, R. A. Gopinath, and H. Guo. *Introduction to Wavelets and Wavelet Transforms*. Prentice Hall, 1997.

[7] P. J. Burt and E. H. Adelson. The Laplacian pyramid as a compact image code. *IEEE Trans. Commun.*, 31:532540, April 1983.

[8] C. Chui and W. He. Compactly supported tight frames associated with refinable functions. *Appl. Comput. Harmon. Anal.*, 8(3):293–319, May 2000.

[9] C. K. Chui, W. He, and J. Stöckler. Compactly supported tight and sibling frames with maximum vanishing moments. *Appl. Comput. Harmon. Anal.*, 13(3):224–262, November 2002.

[10] R. R. Coifman and D. L. Donoho. Translation-invariant de-noising. In A. Antoniadis, editor, *Wavelets and Statistics*. Springer-Verlag Lecture Notes, 1995.

[11] I. Daubechies. *Ten Lectures On Wavelets*. SIAM, 1992.

[12] I. Daubechies, B. Han, A. Ron, and Z. Shen. Framelets: MRA-based constructions of wavelet frames. *Appl. Comput. Harmon. Anal.*, 14(1):1–46, January 2003.

[13] M. N. Do and M. Vetterli. Framing pyramids. *IEEE Trans. on Signal Processing*, 51(9):2329–2342, September 2003.

[14] D. Donoho, M. R. Duncan, X. Huo, and O. Levi. Wavelab 802, 1999. `http://www-stat.stanford.edu/~wavelab/`.

[15] B. Han and Q. Mo. Symmetric MRA tight wavelet frames with three generators and high vanishing moments. *Appl. Comput. Harmon. Anal.*, 18(1):67–93, January 2005.

[16] O. Herrmann. On the approximation problem in nonrecursive digital filter design. *IEEE Trans. on Circuit Theory*, 18(3):411–413, May 1971. Also in [24].

[17] Q. Jiang. Parameterizations of masks for tight affine frames with two symmetric/antisymmetric generators. *Adv. Comput. Math.*, 18:247–268, February 2003.

[18] N. G. Kingsbury. Image processing with complex wavelets. *Phil. Trans. Royal Society London A*, September 1999.

[19] N. G. Kingsbury. Complex wavelets for shift invariant analysis and filtering of signals. *Appl. Comput. Harmon. Anal.*, 10(3):234–253, May 2002.

[20] M. Lang, H. Guo, J. E. Odegard, C. S. Burrus, and R. O. Wells, Jr. Noise reduction using an undecimated discrete wavelet transform. *IEEE Signal Processing Letters*, 3(1):10–12, January 1996.

[21] J. M. Lewis and C. S. Burrus. Approximate continuous wavelet transform with an application to noise reduction. In *Proc. IEEE Int. Conf. Acoust., Speech, Signal Processing (ICASSP)*, volume 3, pages 1533–1536, May 1998.

[22] A. Petukhov. Explicit construction of framelets. *Appl. Comput. Harmon. Anal.*, 11(2):313–327, September 2001.

[23] A. Petukhov. Symmetric framelets. *Constructive Approximation*, 19(2):309–328, January 2003.

[24] L. R. Rabiner and C. M. Rader, editors. *Digital Signal Processing*. IEEE Press, 1972.

[25] A. Ron and Z. Shen. Affine systems in $L_2(\mathbb{R}^d)$: The analysis of the analysis operator. *Journal Funct. Anal.*, 148:408–447, 1997.

[26] A. Ron and Z. Shen. Construction of compactly supported affine frames in $L_2(\mathbb{R}^d)$. In K. S. Lau, editor, *Advances in Wavelets*. Springer Verlag, 1998.

[27] I. W. Selesnick. The double density DWT. In A. Petrosian and F. G. Meyer, editors, *Wavelets in Signal and Image Analysis: From Theory to Practice*. Kluwer, 2001.

[28] I. W. Selesnick. Smooth wavelet tight frames with zero moments. *Appl. Comput. Harmon. Anal.*, 10(2):163–181, March 2001.

[29] I. W. Selesnick. The double-density dual-tree discrete wavelet transform. *IEEE Trans. on Signal Processing*, 52(5):1304–1314, May 2004.

[30] I. W. Selesnick and A. F. Abdelnour. Symmetric wavelet tight frames with two generators. *Appl. Comput. Harmon. Anal.*, 17(2):211–225, 2004.

[31] M. J. Shensa. The discrete wavelet transform: Wedding the à trous and Mallat algorithms. *IEEE Trans. on Signal Processing*, 40(10):2464–2482, October 1992.

[32] E. P. Simoncelli, W. T. Freeman, E. H. Adelson, and D. J. Heeger. Shiftable multi-scale transforms. *IEEE Trans. Inform. Theory*, 38(2):587–607, March 1992.

[33] J.-L. Starck, M. Elad, and D. L. Donoho. Redundant multiscale transforms and their application for morphological component analysis. *Advances in Imaging and Electron Physics*, 132, 2004.

[34] P. Steffen, P. Heller, R. A. Gopinath, and C. S. Burrus. Theory of regular M-band wavelet bases. *IEEE Trans. on Signal Processing*, 41(12):3497–3511, December 1993.

[35] Y.-P. Wang, Q. Wu, K. Castleman, and Z. Xiong. Chromosome image enhancement using multiscale differential operators. *IEEE Trans. Medical Imaging*, 22(5):685–693, May 2003.

[36] G. V. Welland and M. Lundberg. Construction of compact p-wavelets. *Constructive Approximation*, 9(2-3):347–370, June 1993.

[37] Z. Xiong, M. T. Orchard, and Y.-Q. Zhang. A deblocking algorithm for JPEG compressed images using overcomplete wavelet representations. *IEEE Trans. Circuits Syst. Video Technol.*, 7(2):433–437, April 1997.

Ivan W. Selesnick received the B.S., M.E.E., and Ph.D. degrees in Electrical and Computer Engineering in 1990, 1991, and 1996, respectively, from Rice University, Houston, TX. In 1997, he was a visiting professor at the University of Erlangen-Nürnberg, Germany. Since 1997, he has been with the Department of Electrical and Computer Engineering at Polytechnic University, Brooklyn, New York, where he is currently an Associate Professor. His current research interests are in the area of digital signal processing and wavelet-based signal processing.

Dr. Selesnick received a DARPA-NDSEG fellowship in 1991. His Ph.D. dissertation received the Budd Award for Best Engineering Thesis at Rice University in 1996 and an award from the Rice-TMC chapter of Sigma Xi. He received an Alexander von Humboldt Fellowship in 1997, and a National Science Foundation Career award in 1999. In 2003, he received a Jacobs Excellence in Education Award from Polytechnic University. He is currently an associate editor of the IEEE Transactions on Image Processing.